EXPERIMENTAL EVALUATION OF DRAG COEFFICIENT FOR FALLING SPHERE IN NEWTONIAN AND NON-NEWTONIAN FLUID

W.K., Mikhelf[1], and H.Y., Mahmood[2]

[1,2]Department of Mechanical Engineering,
College of Engineering, Baghdad University, Baghdad, Iraq.

Email: [*1]wasaneng87@gmail.com; [2]Hussain_yousif2001@yahoo.com

ABSTRACT: The present study investigated the effect of drag coefficient (C_D) in Newtonian and non-Newtonian fluids which were the rheological properties, size particles. Experiments were conducted using two types of drilling fluids, water represented Newtonian fluid and suspension of bentonite represented non-Newtonian fluid. Stainless steel spheres were used as falling particles. A plastic transparent cylinder of 200 mm inner diameter and 1850 mm length was used as a column for fluid container. Metal particle dedicator was designed and constructed with FPGA kit to perform the experimental work as electronic system to record accurate time of falling particles and high speed camera (1000fps) was also used in order to enhance results. A CFD software ANSYS FLUENT 15.0 was utilized. The study showed drag coefficient (C_D) and particle Reynolds' number (R_{eP}) relationship and the effect of rheological properties on this relationship. The drag coefficient decreased with increasing particles Reynolds number in laminar slip regime in non-Newtonian fluid while remained approximate constant in fully turbulent regime in Newtonian Fluid. Smaller particles showed lower drag coefficient and higher Reynolds numbers for the same material. The range of Reynolds Number was (1.4 *104 < Re < 7.1 *104) and the range of drag coefficient was (0.39 – 0.41) for tap water whereas for the suspension of bentonite, the range of Reynolds Number was (48 < Re < 260) and the range of drag coefficient was (0.64 < CD < 0.76).

KEYWORDS: *Reynolds Number, Drag Coefficient, Newtonian Fluid, Non-Newtonian Fluid, Sphere Particle*

1.0 INTRODUCTION

Motion of particles through a fluid with Newtonian and non-Newtonian rheological properties is a well-studied problem with a broad range of practical application. In Newtonian fluid, the particle motion is applied

to the mechanism of controlling the path, position, direction, physical behavior of particles or velocity. It plays a crucial role in biochemical and chemical engineering because of its several

physical realization, i.e., fluidization of solid, suspension, sedimentation, lubricated transport, slurries, hydraulic fracturing of reservoir and others [1]. The development of new technologies in the materials processing chemical engineering has presented new challenges for fluid dynamics research. This scenario is attributed to advances in geophysical fluid dynamics focusing on complex fluids including slurries [2], coastal sediments [3], polymer flows in petroleum reservoirs [4], landslide geometrical [5] and liquefied soils created following earthquakes [6]. Other authors have focused on biomechanics of plasma and blood fluids in the past numerous decades [7]. Such fluids show a flow behavior that could be described by Newtonian relationships so it is referred as non-Newtonian fluids. Particles Reynolds' number is to indicate whether the boundary layer around a particle is turbulent or laminar, and the drag exerted depends on this. It is a measure of the relative importance of inertial to viscous forces of flow, and the ratio is given as follows:

For Newtonian fluid:

$$Re_p = \frac{\rho_f \vartheta D}{\mu} \quad (1)$$

For Non-Newtonian fluid power law:

$$Re_p = \frac{\rho_f \vartheta^{2-n} D^n}{K} \quad (2)$$

When R*ep* is particle Reynolds number, is Density of fluid, ϑ is Velocity of particle, D is equivalent diameter, μ is Viscosity of fluid, n is Flow behavior index and k is Consistency index [8]. Solid particles settling in drilling fluids has been one of the major problems in an effective removal of drilled cuttings from the bit to the surface for a profitable drilling operation. Therefore, it will take two type of drilling mud, water as Newtonian and suspension of bentonite as non-Newtonian fluid. Both fluids are taken because they are the most commonly used fluid in-oil wells. Drag coefficient is determined experimentally for the motion of different configuration through a cylindrical column filled by suspension of bentonite (30% of bentonite and 70% of water); the experiments will be repeated with water and the results will be compared with previous studies. In the present work, spheres are used as falling particles. The focus of the present study was on drag coefficient versus particle Reynolds number for free falling particles.

1.1 The Scope of this Work

The study analyzes the effect of drag coefficient (CD) in Newtonian and non-Newtonian fluids which were the rheological properties, size particles. Besides, the results were plotted with Reynolds number to find new correlations. A plastic transparent cylinder of 200 mm inner diameter and 1850 mm length was used as a column for fluid container. Metal particle dedicator (consisted of two coils tied to electronic circuit) was designed and constructed with FPGA kit to perform the experimental work as an electronic system to record accurate time of falling particles. A high speed camera (1000fps) was used. Column was filled with two types of drilling fluid sequentially; Newtonian fluids using water and non-Newtonian fluids using suspension of bentonite. Different stainless steel particles shapes [sphere (1.1 cm ≤ D ≤ 0.3 cm), cylinder (1.3 cm ≤ l ≤ 3.2 cm), cube (1 cm ≤ l ≤ 3 cm) and cone (1 cm ≤ h ≤ 3 cm)] were used and releasing particles apparatus was used for falling them freely in the column with two types of drilling fluids.

2.0 PREVIOUS STUDIES

2.1 Newtonian fluid

Gilbert et al. [9] propose a three-parameter equation just before correlate the drag coefficient and the particle Reynold number. A third parameter is introduced in addition to the two parameters given by Stokes.

$$C_D = XRe^y + Z \tag{3}$$

Turton and Levenspiel [10] introduce two equations (4) and (5) to correlate the drag coefficient and particle Reynolds number for falling spheres. These two equations are similar to the original three-parameter model by Gilbert et al. [9].

$$C_D = 27.2Re_p^{0.827} + 0.427 \; for \; Re < 2 * 10^5 \tag{4}$$

$$C_D = \frac{24}{Re_p}(1 + 0.173Re_p^{0.657} + \frac{0.413}{1+16300\, Re_p^{-1.09}} \; for \; Re < 2 * 10^6 \tag{5}$$

Haider and Levenspiel [11] propose four-parameter general drag coefficient-Reynolds number relationship for spherical particle, as Equation (6),

$$C_D = \frac{24}{Re_p}\left(A + Re_p^B\right) + \frac{C}{1+\frac{D}{Re_p}} \tag{6}$$

The experimental data used to find the best values of the four parameters is similar to Turton and Levenspiel [10] the final equation obtained for the drag coefficient for sphere is as follows:

$$C_D = \frac{24}{Re_p}\left(0.1806 + Re_p^{0.6459}\right) + \frac{0.4251}{1+\frac{6880.95}{Re_p}} \quad (7)$$

Morrison (2013) finds new data correlation for drag coefficient for sphere simple formula [12]. Equation is as follows:

$$C_D = \frac{24}{Re} + \frac{2.6(\frac{Re}{5})}{1+(\frac{Re}{5})^{1.52}} + \frac{0.411(\frac{Re}{263000})^{-7.94}}{1+(\frac{Re}{263000})^{-8}} + \frac{Re^{0.8}}{461000} \quad (8)$$

Where Re is the Reynolds number and CD is the drag coefficient.

2.2 *Non-Newtonian Fluid*

Darby [13] predicts the resulting expression that provide an accurate representation of the drag in non-Newtonian fluids on state that (A) and (B) made dependent on the power law index (n).

$$C_D = \left(\frac{A}{\sqrt{R_e}} + B\right)^2 \quad (9)$$

$$A = 4.8\left(\frac{1.33 + 0.37n}{1 + 0.7n^{3.7}}\right)^{1/2} \quad (10)$$

$$B = \left[\left(\frac{1.82}{n}\right)^8 + 34\right]^{1/8} \quad (11)$$

Kelessidis [14] predicts the resulting drag coefficient correlation for power law fluid.

$$C_D = \frac{24}{Re_{gn}}\left[1 + 0.1466 {Re_{gn}}^{0.378}\right] + \frac{0.44}{1 + 0.2635/Re_{gn}} \quad (12)$$

For $0.1 < Re_{gn} < 103$

Yousif [15] investigates the surface roughness effect of falling spheres in different fluids (Newtonian and non-Newtonian) on the virtual mass coefficient for single sphere, two spheres sides by side and on line movement. A glass cylinder of 220 mm diameter and 1500 mm length is used as a liquid column. A new design and contraction system for falling spheres are used, demonstrating a perfect falling of the spheres. Two types of measuring velocities are used; the FPGA kit (as electronic

system) and high-speed camera (Samsung 3000 / 1000 fps) as virtual method.

3.0 EXPERIMENTAL WORKS

This suspension was prepared by adding 30 g of bentonite powder to letter of tap water. A mixer was used to mix the required suspension for each batch for about 10 minutes. This procedure was repeated to get about 58 L. of this suspension (the size of the cylindrical column). Fanning viscometer type OFITE [model 800] which had eight speeds (600, 300, 200, 100, 60, 6, and 3 rpm) was used to find the viscosity of the suspension. Density was measured using mud balance type OFITE. The power law constants can be calculated from the equation used [16].

$$n = 3.32\,X\,\log\frac{600\,.rpm\,.reading}{300\,.rpm\,.reading}$$

$$\mu_a = \frac{600\,.rpm.reading}{2}$$

$$K = \frac{600\,.rpm.reading}{(1022)^n}$$

Where n = flow behavior index, K = Consistency index, μa = Apparent viscosity. The physical properties are as follows:

n=0.2318 k= 2.02 (pa.sn) μ_a = 4 (c.p) ϱ= 1020 (Kg/m^3)

3.1 Equipment

The experimental device and the instruments were designed and constructed in the Heat Transfer lab, at the mechanical Engineering Department / University of Baghdad and circumstances of experience were under standard conditions. The experimental device consisted of Plastic Transparent column of 1850 mm long and 200 mm inner diameter with 5 mm thickness. The column was applied with flanged ends. The bottom end closed with a flange of spherical shape. This flange was supplied with a valve for drain. The cylindrical column fixed well on a rigid steel structure. The column leveled horizontally at its open end. The effective length of column was kept 1000 mm between the top and bottom and at 200 mm diameter. Electronic system and high-speed camera 1000 FP were set to determine accurate time of falling

sphere. Releasing Particles apparatus was also used. Figure 1 shows the experimental device in the Lab with suspension of bentonite.

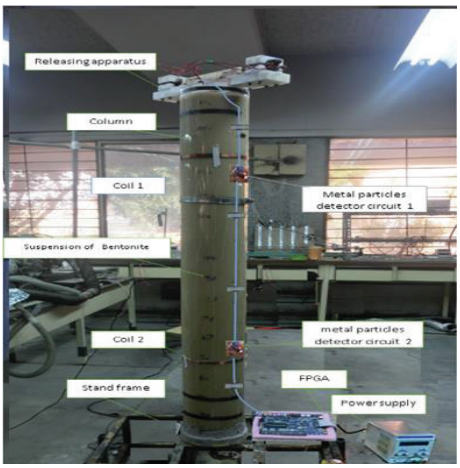

Figure 1: The experiment device in the lab with suspension of bentonite

Figure 2: Coil of metal particles detector

3.2 Electronic System

Many attempts have been made to test electronic systems such as arrangements to experience the number of laps for coil. The principle of electromagnetic training is the variable magnetic field created to produce the variable current through an inductor coil prepared from coated copper wire (30 SWG). The current had to be supplied through an oscillator circuit which used the TDA0161 proximately detector IC [17]. These monolithic integrated circuits were designed for metallic body detection using inductor coil and operated while sensing variations on high eddy frequency current losses. By using an externally tuned circuit, it acted as oscillators; the output signal level was altered when approaching a metallic object. Each inductor coil had a mean diameter of 20 cm, a mean thickness of 0.7 cm and 34 turns as shown in Figure 2.When the metal object was detected using the TDA0161 IC, a signal was received as an output from a switching circuit created with the

BC547 transistor. LED was used as a visual aid to recognize whether the metal objects had detected any plate. The metal detector method needs calibration. Previously, it was done using its inbuilt variable resistors. The 10 kΩ variable resistor was used for coarse tuning while the 1 kΩ variable resistor for well tuning. In this process, 10 kΩ resistor was kept at zero resistance position and the 1 kΩ resistor in full resistance location. 10 kΩ resistor was turned clockwise (to increase resistance) until the green LED was turned off. At this point, the 1 kΩ resistor was turned counter clockwise until the LED was just about to light. Then, the reset button was pressed to adjust the 1 kΩ resistor to its optimal detection position within an acceptable error of 0.4%. The readings of high-speed camera were less accurate than those recorded by FPGA.

4.0 RESULTS AND DISCUSSION

4.1 Newtonian Fluid (Water)

4.1.1 Behavior of Settling Velocity

Figure 3 shows relationship of (ϑ-D) for falling Sphere in water. For free falling sphere, the velocity increased as the diameter of the sphere increased. The large particles diameter gave the highest terminal velocity than smaller particles. The reason could be the large particles have the largest weight and are less affected by viscous force and buoyancy force opposing the settling speed; therefore the large particle moved faster than smaller ones.

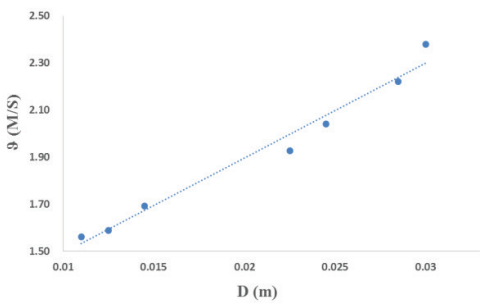

Figure 3: Relationship of (ϑ-D) for falling sphere in water

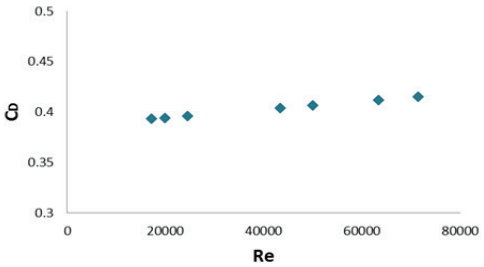

Figure 4: Relationship (CD-Re) for falling sphere in water

4.1.2 Behavior of Drag Coefficient

The range of Reynolds Number (1.4 *104 < Re < 7.1 *104) was used in water and the range of drag coefficient was (0.39 – 0.41) for sphere. From Figure 4, can be seen the drag coefficient increased with the Reynolds number, but this increase was very little or approximately constant. As a result, the flow around the falling particle was fully turbulent. Hence, when the turbulent slip regime started, the drag coefficient was at a constant value due to the fact that the inertial forces dominated this region and viscous forces had a small effect; as previously mentioned drag is essentially independent of viscous force and therefore, the Reynolds Number in this zone is independent. The variety in drag coefficient (CD) occurs only in a response to change in particle shape.

The values of drag coefficient were high at low values of Reynolds' number and as Reynolds' number increased the drag coefficient decreased, because the viscous forces dominated the laminar-slip regime. When this region ended and the transition-slip regime started, the effect of Reynolds' number on drag coefficient decreased, until the turbulent-slip regime started and the drag coefficient was at a constant value because the inertial forces dominated this region and viscous forces had little effect. For this reason, the increase in Reynolds' number will not decrease the drag coefficient [18].

4.2 Non-Newtonian Fluid (Drilling Mud)

4.2.1 Behavior of Settling Velocity

For free falling sphere, the velocity increased as diameter of the sphere increased. Figure 5 shows the relationship between velocity and diameter for falling sphere in suspension bentonite. As the case in the Newtonian fluids, when the particle diameters increased, the velocities of falling particle in non-Newtonian fluids increased but this increase is less of falling particles in the Newtonian fluid, because the drag

force exerted by fluid of the particles increased due to the viscosity of suspension of bentonite which was more than water viscosity.

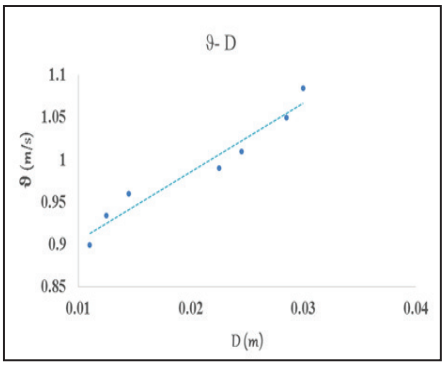

Figure 5: Relationship between velocity and diameter for falling sphere in suspension bentonite

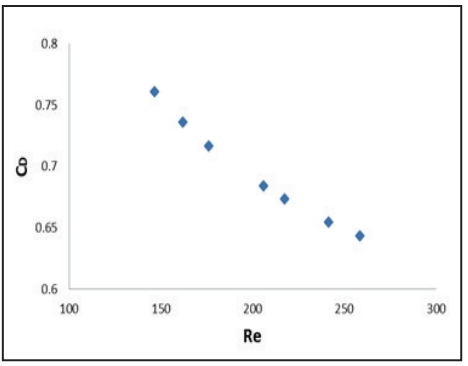

Figure 6: Relationship between drag coefficient and Reynolds Number sphere in suspension bentonite

4.2.2 *Behavior of Drag Coefficient*

Using correlation [14], the results of the relationship drag coefficient with Reynolds number were obtained. Hence, drag coefficient decreased as the Reynolds number increased. Figure 6 shows the relationship between drag coefficient and Reynolds Number sphere in suspension bentonite. When flow behavior index (n) was less than unity the drag coefficient would increase because the particles were falling at lower velocity; and this effect was greatly realized through low values of Reynolds 'number [18]. The range of Reynolds Number was ($48 < Re < 260$) and the range of drag coefficient was ($0.64 < CD < 0.76$) for sphere.

As a result, the flow around the falling particle was laminar, so when the laminar slip regime started, the drag coefficient would decrease due to the fact that the viscous forces dominated this region as previously mentioned and flow behavior index (n) was less than unity. Figures 7 to 10 ANSYS FLUENT15.0 describes the falling spheres in both fluid water and suspension of bentonite in the boundary layer was higher when spheres were falling in suspension of bentonite because of the higher viscosity.

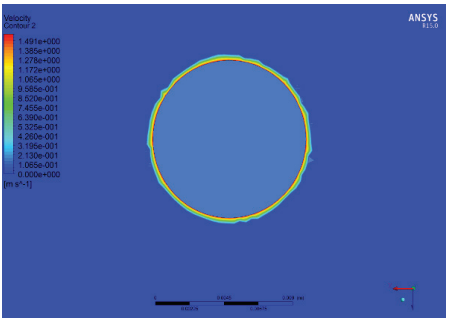

Figure 7: Falling sphere with diameter 1 cm in water

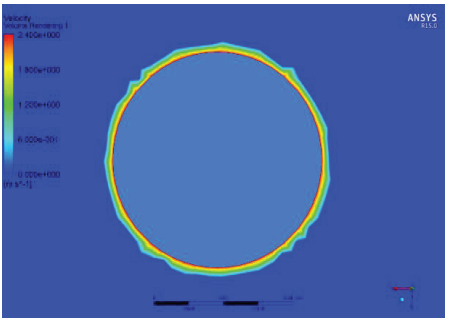

Figure 8: Falling sphere with diameter 3 cm in water

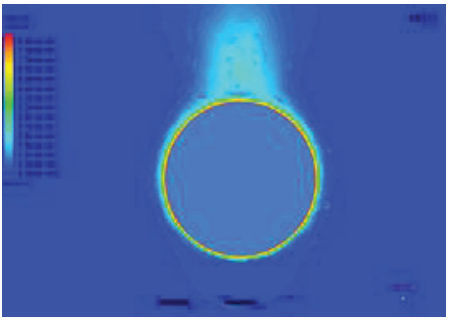

Figure 9: Falling sphere with diameter 1 cm in Bentonite suspension

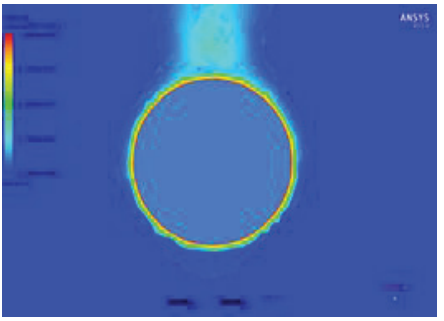

Figure 10: Falling sphere with diameter 3 cm in Bentonite suspension

5.0 DISCUSSION

The results of variation drag coefficient with Reynolds Number are compared with existing studies as shown below:

1. For falling spherical particles in Newtonian fluid, the graph between drag coefficient and Reynolds number of present work resembles Marrison [13] as shown in Figure 11.

The correlations of Marrison [12] covers a wide range of Reynolds number which show different regions in (CD – Re) graph and the turbulent slip regime (Re > 104) the drag coefficient is approximate constant, which is proved in present work for the Reynolds number range is (1.4 *104 < Re < 7.1 *104).

2. For falling spherical particles in non-Newtonian fluid, the graph between drag coefficient and Reynolds number of present work resembles Kelessidis [12] as shown in Figure 12.

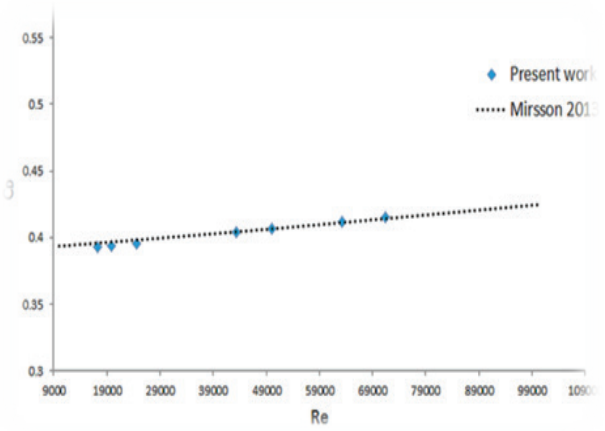

Figure 11: Comparison relationship between Reynolds Number and drag coefficient for falling sphere between Marrison [13] and present work

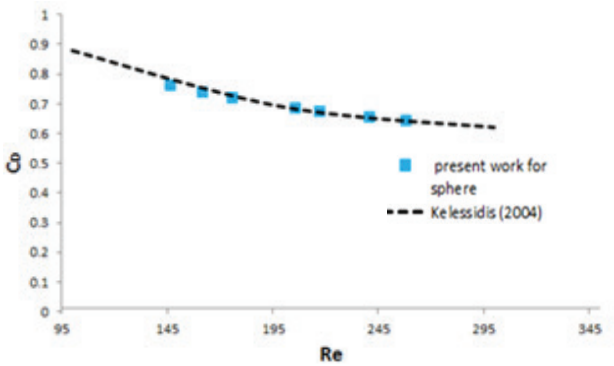

Figure 12: Comparison of relationship between Reynolds number and drag coefficient for falling sphere between Kelessidis and present work for suspension of bentonite

6.0 CONCLUSION

Drag coefficient is influenced by turbulent regime or laminar regime, particle sizes and fluid properties. The experiment yields that the terminal velocities of particle increase with the increase of particle diameter for the same material in Newtonian fluid and non-Newtonian fluid.

6.1 Newtonian Fluid

- Drag coefficient passes in turbulent slip regime.
- The drag coefficient is approximate constant.
- Drag coefficient depends on Reynolds number.
- When particle Reynolds number increases, the drag coefficient of particle will decrease.

6.2 Non-Newtonian Fluid

- Drag coefficient in non-Newtonian fluid passes in laminar slip regime.
- When particle Reynolds number increases, the drag coefficient of particle will decrease.
- The rheological properties of non-Newtonian fluids have a great effect on drag coefficient, because as the fluid becomes far from Newtonian behavior, (flow index, n, far from unity), the drag coefficient will increase.

REFERENCES

[1] J. Dinesh, Modelling and Simulation of a Single Particle in Laminar Flow Regime of a Newtonian Liquid. Gujarat, India: Alpha Project Services, 2009.

[2] H. E. Brenner, Interfacial Transport Processes and Rheology. MIT Mass: USA, 1991.

[3] P. L. Liu, "Long Waves in Shallow Water over a Layer of Bingham Plastic Fluid Mud," *Int. J. Eng. Sci: Physical Aspects*, 1933.

[4] S. E. Rodriguez, "Flow of Polymer Solutions Through Porous Media," *J. Non-Newton Fluid Mech*., 1993.

[5] C. J. Philips, "*Determining Rheological Parameters of Debris Flow Material*," Geomorphology, 1991.

[6] J. A. Locat, "Viscosity, Yield Stress, Remoulded Strength and Liquidity Index Relationships For Sensitive Clays," *Can. Geotech. J*., 1988.

[7] C. K. Kang, "The Effects of Microstructure on the Rheological Properties of Blood," *Bull. Math. Biol*., 1976.

[8] G. J. Clift et al, Bubbles, Drops and Particles. New York: Academic Press, 1978.

[9] L. D. Gilbert et al., "Altman, Velocity lag of particles in linearly accelerated combustion gases," *Jet Propulsion*, 1955.

[10] R. Turton, and O. Levenspiel, "A Short Note on the Drag Correlation for Spheres," *Powder Technology*, 1986.

[11] Haider and H. Levenspiel, "Drag Coefficient and Terminal Velocity of Spherical and Nonspherical Particles," *Powder Technology*, 1989.

[12] F. A. Morrison, Data Correlation for Drag Coefficient for Sphere. Houghton: Michigan Technological University, 2013.

[13] Darby, Fluid Dynamics. Canada: Addison-Wesley Publishing Company, Inc., 1996.

[14] Kelessidis, "Measurements and Prediction of Terminal Velocity Of Solid Spheres Falling Through Stagnant Pseudoplastic Liquids," *J. of Powder Technology*, 2004.

[15] H. Yousif. Experimental Evaluation of the Virtual Mass and Roughness of Solid Particles Accelerating in Newtonian and Non-Newtonian Fluids. Baghdad: University of Baghdad, 2012.

[16] H. Rabia, Petroleum Drilling Rigs. *Hydraulic Engineering*, Newcastle: Athenaeum Press, 1989.

[17] STMicroelectronics. TDA0161 Datasheet. [online]. Available: http://www.st.com/internet/com/TECHNICAL_RESOURCES/TECHNICAL_LITERATURE/DATASHEET/CD00000119.pdf.

[18] A. R. Muhannad, "The Effect of Particles Shape and Size and the Rheological Properties of Non-Newtonian Fluids on Drag Coefficient and Particle Reynold's Number Relationship," Baghdad: Baghdad University, 2013.